Long Polaron Lifetime in InAs/GaAs Self-Assembled Quantum Dots

S. Sauvage and P. Boucaud*
Institut d'Electronique Fondamentale, Bâtiment 220, Université Paris-Sud, 91405 Orsay, France

R. P. S. M. Lobo
CLIO/LURE, Bâtiment 209 D, Université Paris-Sud, 91405 Orsay, France

F. Bras and G. Fishman
Institut d'Electronique Fondamentale, Bâtiment 220, Université Paris-Sud, 91405 Orsay, France

R. Prazeres, F. Glotin, and J. M. Ortega
CLIO/LURE, Bâtiment 209 D, Université Paris-Sud, 91405 Orsay, France

J.-M. Gérard
CEA-Grenoble, DRFMC-PSC, 38054 Grenoble Cedex 9, France
(Received 14 December 2001; published 12 April 2002)

We have investigated the polaron dynamics in n-doped InAs/GaAs self-assembled quantum dots by pump-probe midinfrared spectroscopy. A long T_1 polaron decay time is measured at both low temperature and room temperature, with values around 70 and 37 ps, respectively. The decay time decreases for energies closer to the optical phonon energy. The relaxation is explained by the strong coupling for the electron-phonon interaction and by the finite lifetime of the optical phonons. We show that, even for a large detuning of 19 meV from the LO photon energy in GaAs, the carrier relaxation remains phonon assisted.

DOI: 10.1103/PhysRevLett.88.177402 PACS numbers: 78.67.Hc, 71.38.–k, 78.47.+p, 82.53.Mj

The relaxation of carriers in semiconductor quantum dots has been widely debated in literature in recent years. In bulk or two-dimensional heterostructures, it is well known that the interaction between carriers and longitudinal-optical (LO) phonons through the Fröhlich coupling provides an efficient relaxation path for carriers, with typical relaxation times in the ps range. Because of the discrete density of states in quantum dots, it was predicted that the LO-phonon-assisted relaxation would be quenched for energies different from the LO-phonon energy [1]. The prediction of an inefficient phonon scattering based on energy conservation arguments was referred to as the phonon bottleneck in the literature [2]. Multiphonon relaxation paths involving LO phonons and longitudinal acoustical (LA) phonons through the deformation potential interaction were considered using a second-state perturbation calculation [3]. It was shown that these two-phonon processes could enlarge, by only a few meV, the spectral window where an efficient relaxation of the carriers would occur. Auger-assisted relaxation mechanisms were also discussed as an efficient scattering mechanism at large carrier densities [4].

Recently, Inoshita *et al.* pointed out that the perturbative treatment using the Fermi golden rule for the electron-phonon interaction should not apply for quantum dots [5]. The strong coupling of electrons and phonons leads to the formation of coherent admixtures between electrons and phonons, the polarons. The formation of polarons in InAs/GaAs self-assembled quantum dots was experimentally evidenced by magneto-optical absorption experiments with n-doped InAs/GaAs self-assembled quantum dots [6]. The coherent electron-phonon interaction has led several authors to reconsider the carrier relaxation in quantum dots. Li *et al.* have emphasized that the finite lifetime of the optical phonons due to the crystal anharmonicity should lead to an efficient relaxation even for large detuning from the optical phonon energy [7,8]. Verzelen *et al.* have developed a microscopic model for the polaron states in quantum dots using the Fröhlich Hamiltonian [9]. A density matrix treatment of the polaron relaxation was performed. These authors have shown that, in an energy window around the optical phonon energy, the energy relaxation was triggered by phonon-phonon interactions on polaron states. Verzelen *et al.* [9] have pointed out that their microscopic approach, as compared to a semiclassical treatment of the polaron like the one proposed by Li *et al.* [8], leads to similar values for the electronic relaxation in an energy window of 8 meV around the LO-phonon energy. Outside this window, a drastic difference occurs: Verzelen *et al.* predict a quenching of the relaxation while Li *et al.* predict a monotonic variation of the relaxation time as a function of the energy detuning.

Experimentally, most of the studies on the intradot relaxation were performed using an interband optical pumping [10,11]. A fast relaxation was usually observed, and the intradot carrier relaxation was generally linked to electron-hole scattering and Auger-type processes at high excitation power densities. Recently, an observation of a

phonon bottleneck in the quantum dot electronic relaxation was reported at low temperature [12]. Similar slowing of the relaxation attributed to charge separated quantum dots was already reported for CdSe nanocrystals [13].

In this Letter, we report on the first measurement of the polaron decay measured with an intersublevel excitation in *n*-doped InAs/GaAs self-assembled quantum dots. The relaxation is studied by midinfrared pump-probe spectroscopy as a function of the excitation energy and as a function of the temperature. Long polaron decay times T_1 are interpreted in the framework of a *strong* coupling for the electron-phonon interaction. They show a significant phonon bottleneck for the intradot electronic relaxation as compared to bulk or two-dimensional materials. They also show that the coupling to optical phonons remains the dominant relaxation mechanism even for large intersublevel detuning from the phonon energy. The relaxation of the polaron is driven by the finite lifetime of the optical phonons associated with the crystal anharmonicity.

The investigated sample consists of 30 InAs quantum dot layers separated by 50 nm thick GaAs barriers [14]. The dot density is around 4×10^{10} cm^{-2}. A nominal doping of two carriers per dot was provided by a delta-planar doping 2 nm below the quantum dot layers. The dots have a flat elliptical lens-shaped geometry with a typical dot height of 2.5 nm and a base length of 25 nm. The midinfrared pump-probe experiments were performed with the picosecond free-electron laser CLIO (Centre Laser Infrarouge d'Orsay) [15]. The pump and probe signals injected close to the normal incidence on the sample were detected with liquid-nitrogen cooled long wavelength mercury-cadmium-telluride photodetectors. The pump was spatially separated from the probe with an angle of 20°. The residual pump signal seen by the probe detector was around 1:100. The probe was not as focused as the pump. This results in an incomplete spatial overlap which limits the amplitude of the absorption change. A mechanical chopper synchronized with the free-electron laser macropulse repetition rate was inserted in the optical path of the pump beam. The signal-to-noise ratio of the measurement was improved by normalizing the probe signal between two successive macropulses with or without the pump signal. This technique allows one to perform very sensitive measurements with typical noise of 0.4% for accumulation times for a few seconds.

Figure 1 shows the low temperature (5 K) absorption spectrum associated with the optical transition between the *s*-like conduction ground state and the *p*-like first conduction excited state, the so-called "*s*-*p*" intersublevel transition. This intersublevel transition is in-plane polarized. The absorption was measured with the sample at normal incidence and a polarized light along the $[\bar{1}10]$ direction. The *s*-*p* transition exhibits two resonances [16] at 56 and 63 meV observed for light polarized along $[\bar{1}10]$ and $[110]$ as a consequence of the dot elongation along the $[\bar{1}10]$ direction. The low-energy transition at 56 meV presents a 6 meV broadening (full width at half maximum) associated with the dot size fluctuation and a 8.8% absorption amplitude. The small linewidth can be explained by the small dependence of the intersublevel transition energy as a function of the dot size [17]. The 8.8% amplitude corresponds to an average population of 1.2 carriers per dot for a calculated dipole matrix element of 3.4 nm. The confined states in the quantum dots were obtained in the framework of a three-dimensional 8 band $\mathbf{k} \cdot \mathbf{p}$ calculation. The strain tensor is assumed constant within the InAs dot volume and equal to the one of an InAs quantum well grown on a GaAs substrate. The GaAs barriers are assumed unstrained. A 25 nm × 28 nm × 2.5 nm elliptical quantum dot exhibits in-plane polarized intersublevel transitions at 56 and 63 meV, thus demonstrating a reasonably good agreement between the structural measurements and the experimental measurements. We note that the resonance energy of this intersublevel transition is detuned by around 20 meV from the GaAs LO-phonon energy (36 meV). For this detuning, the strong coupling between electron and phonons should modify the resonance energy obtained without accounting for this coupling by less than 3 meV [9]. We emphasize that the choice of a unipolar excitation for the study of the intradot relaxation offers four advantages: (i) only electrons (i.e., no holes) are involved; (ii) the average carrier population of the dots is lower than two; i.e., Auger-assisted relaxation is not expected to dominate; (iii) the *s*-*p* intersublevel transition corresponds to a transition with well-isolated conduction states, and there are no intermediate electronic states, in a single particle description, to assist the relaxation; (iv) the inhomogeneous broadening of this intersublevel transition allows the study of the relaxation rate for different energy differences.

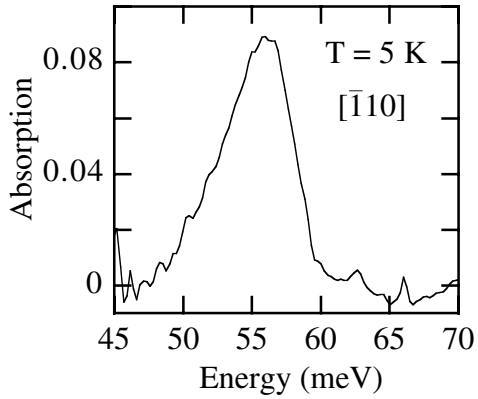

FIG. 1. Low-temperature (5 K) infrared absorption of the *n*-doped quantum dot sample. The infrared light polarized along the $[\bar{1}10]$ direction is injected along [001] with the sample at normal incidence. The transmission of the sample is normalized by the transmission of a GaAs substrate with an equivalent thickness.

Figure 2 shows the spectral dependence of the probe transmission as a function of the time delay between the pump and the probe. The spectral dependence is illustrated by excitation energies varying between 54.5 meV (top) and 50.5 meV (bottom). The measurement is

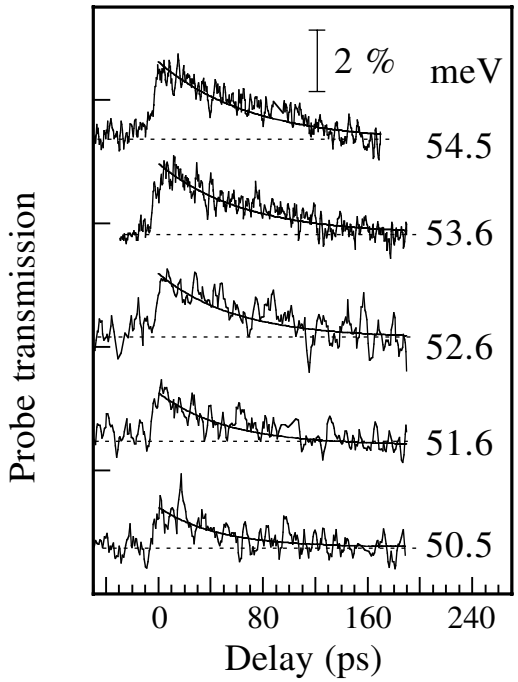

FIG. 2. The 5 K transmission change in linear scale as a function of the time delay between the pump and the probe polarized along the $[\bar{1}10]$ direction for several excitation energies, indicated on the right side of the curve. The curves have been offset for clarity. The baselines are shown as dashed lines. The numerical fits used to extract the decay time are superimposed on the experimental data.

performed at low temperature (5 K) with the free-electron laser polarized along the $[\bar{1}10]$ direction. The decay time was extracted by fitting the absorption recovery at positive time delays with an exponential function. These numerical fits superimposed on the experimental curves are shown in Fig. 2. A small shoulder due to a parasitic reflection in the beam splitter is observed on the absorption profile at time delays between 80 and 140 ps. The signals at these time delays were removed to obtain the numerical fit. We note that the amplitude of the bleaching decreases as the excitation energy is detuned from the intersublevel resonance. Several features are illustrated in Fig. 2. The intraband relaxation measured with this unipolar excitation is long as compared to bulk or two-dimensional systems, with a typical relaxation time of 70 ps for an excitation energy of 54.5 meV. It is a clear illustration of the slowing of the intradot relaxation since this value is much larger than the picosecond relaxation times reported for energy differences above the LO-phonon energy in two-dimensional semiconductors [18]. Meanwhile, no quenching of the relaxation is observed. Quite interestingly, we observe a significant dependence of the relaxation time as a function of the excitation energy, i.e., the energy difference of the confined states. The relaxation time decreases monotonically as the energy level difference gets closer to the optical phonon energy.

In Ref. [8], the electronic carrier relaxation in quantum dots was investigated by considering the strong coupling for the electron-phonon interaction. The carrier relaxation was attributed to the decay of the optical phonon due to the anharmonic coupling of the confined LO phonon to acoustic phonons. The relaxation time can be written in the analytical form following (1):

$$\tau = \frac{1}{\Gamma - \sqrt{2(R - X)}}, \tag{1}$$

where $\Gamma = 1/\tau_{\mathrm{ph}}$ with τ_{ph} the lifetime of the optical phonon, $R = \sqrt{X^2 + Y^2}$ with $X = (g/h)^2 + (\Delta^2 - \Gamma^2)/4$, and $Y = \Gamma\Delta/2$. Δ is the detuning from the phonon energy, h is the Planck constant, and g is the coupling strength of the electron to all LO modes, which accounts for the phonon population. The low-temperature LO-phonon lifetime is taken as the value of bulk GaAs $\tau_{\mathrm{ph}} = 7$ ps [8]. This dependence on the detuning corresponds to a relaxation rate $1/\tau$ which varies as the bulk phonon relaxation rate Γ times the weight of the phonon component in the polaron state. As this weight decreases when the detuning from the LO-phonon energy increases, the relaxation time becomes longer at large detuning. To comply with the experiment, we have adjusted the coupling strength for the electron-phonon interaction. For a cubic quantum dot with a 25 nm size, the coupling strength at low temperature is calculated as $0.35\hbar\omega_0/\sqrt{25}$ where $\hbar\omega_0$ is the optical phonon energy [8]. This coupling strength (2.52 meV) leads to a decay time of 200 ps at 54.5 meV, i.e., to an overestimation by a factor of 3 of the decay time. Figure 3 shows a comparison between the experimental decay time and the calculated decay time at low temperature [19]. The only adjustable parameter is the coupling strength for the electron-phonon interaction, $g = 4.4$ meV in the present case. A very good agreement between experiment and theory is obtained for the spectral dependence of the relaxation time and its decrease as the energy gets closer to the LO-phonon energy. The relaxation time is also well reproduced by considering this stronger coupling strength for the electron-phonon

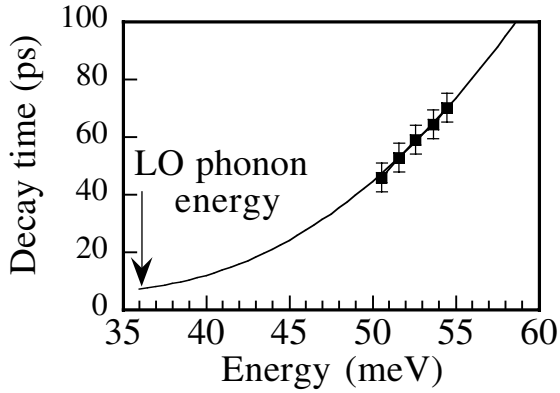

FIG. 3. Spectral dependence of the decay time (squares) at low temperature (5 K) compared to the theoretical dependence by considering the electron-phonon interaction in the strong coupling regime.

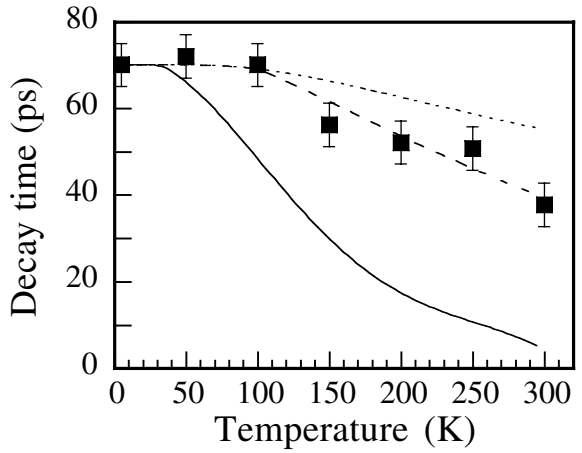

FIG. 4. Temperature dependence of the decay time at 54.5 meV (squares) compared to the theoretical dependence by considering the electron-phonon interaction in the strong coupling regime. The full curve accounts for the theoretical temperature dependence of the LO-phonon lifetime (Ref. [7]), the dashed curve for a constant phonon lifetime of 7 ps up to 100 K and a linear decrease from 100 to 300 K down to 5 ps, and the dotted curve for a constant phonon lifetime of 7 ps.

interaction. Such stronger coupling in self-assembled quantum dots was already reported previously [20]. We emphasize that in the framework corresponding to Eq. (1), solely the electron-phonon interaction is considered for the carrier relaxation. Our data illustrate that the carrier relaxation can be described by the polaron picture, as it was theoretically suggested in Refs. [5] and [8]. The energy relaxation is directly linked to the finite lifetime of the optical phonons and their decay into acoustic phonons due to crystal anharmonicity. We note that, as mentioned in Ref. [9], the microscopic description of the polaron relaxation was expected to be similar to the semiclassical approach of Li *et al.* only in a spectral window of 8 meV around the optical phonon energy. The relaxation was expected to be quenched outside this window since the polaron states are stable entities as eigenvectors of the electron-phonon interaction. The present relaxation values are therefore not well accounted for by the microscopic description reported in Ref. [9], but by the one of Ref. [8].

The absorption change was monitored as a function of the temperature for a fixed excitation energy of 54.5 meV (22.75 μm wavelength). The absorption recovery time decreases as the temperature is increased. The decrease of the relaxation time remains limited, however, and a long relaxation time of 37 ps is still observed at room temperature. Figure 4 shows a comparison between the experimental values of the temperature dependence of the decay time and the calculated dependence of this parameter in the strong coupling regime. The full line accounts for the theoretical description of the phonon lifetime presented in Ref. [7]. This description underestimates the value of the phonon lifetime at high temperature (2.5 ps at room temperature as compared to the 3.5 ps value measured experimentally for bulk GaAs). The dashed line corresponds to a constant LO-phonon lifetime of 7 ps up to 100 K and a linear decrease of the lifetime from 100 to 300 K with a slope of 0.01 ps/K that is a 5 ps lifetime at room temperature. The dotted curve considers a constant phonon lifetime of 7 ps from low temperature to room temperature. In this case, the temperature dependence stems only from the Bose occupation factor which appears in the coupling strength in the electron-phonon interaction. The full line shows a strong dependence of the decay time vs temperature as compared to the experimental measurements. Meanwhile, a constant phonon lifetime (dotted line) is not sufficient to account for the temperature dependence of the decay time. A satisfying agreement is obtained in the intermediate case (dashed line). We emphasize that a difference on the phonon lifetime at room temperature (5 ps instead of 3.5 ps) remains reasonable since the 3.5 ps is related to bulk GaAs while the considered dynamics is related to InAs dots. The data reported in Fig. 4 show that the temperature dependence of the carrier relaxation in quantum dots is driven by the temperature dependence of the LO-phonon lifetime. As the phonon lifetime presents a weak dependence as a function of the temperature, the decay time of the polarons weakly depends on temperature.

*Electronic address: phill@ief.u-psud.fr

[1] U. Bockelmann and G. Bastard, Phys. Rev. B **42**, 8947 (1990).
[2] H. Benisty, C. M. Sottomayor-Torres, and C. Weisbuch, Phys. Rev. B **44**, 10 945 (1991).
[3] T. Inoshita and H. Sakaki, Phys. Rev. B **46**, 7260 (1992).
[4] U. Bockelmann and T. Egeler, Phys. Rev. B **46**, 15 574 (1992).
[5] T. Inoshita and H. Sakaki, Phys. Rev. B **56**, R4355 (1997).
[6] S. Hameau *et al.,* Phys. Rev. Lett. **83**, 4152 (1999).
[7] X-Q. Li and Y. Arakawa, Phys. Rev. B **57**, 12 285 (1998).
[8] X-Q. Li, H. Nakayama, and Y. Arakawa, Phys. Rev. B **59**, 5069 (1999).
[9] O. Verzelen, R. Ferreira, and G. Bastard, Phys. Rev. B **62**, R4809 (2000).
[10] B. Ohnesorge *et al.,* Phys. Rev. B **54**, 11 532 (1996).
[11] V. I. Klimov *et al.,* Phys. Rev. B **60**, 13 740 (1999).
[12] J. Urayama *et al.,* Phys. Rev. Lett. **86**, 4930 (2001).
[13] P. Guyot-Sionnest *et al.,* Phys. Rev. B **60**, R2181 (1999).
[14] S. Sauvage *et al.,* Appl. Phys. Lett. **71**, 2785 (1997).
[15] S. Sauvage *et al.,* Phys. Rev. B **59**, 9830 (1999).
[16] S. Sauvage *et al.,* Phys. Rev. B **63**, 113312 (2001).
[17] T. Brunhes *et al.,* Phys. Rev. B **61**, 5562 (2000).
[18] M. C. Tatham, J. F. Ryan, and C. T. Foxon, Phys. Rev. Lett. **63**, 1637 (1989).
[19] The error bars of 10 ps shown in Figs. 3 and 4 correspond to a typical variation of the extracted time between successive measurements. The error bar, estimated on the large amplitude curves, is displayed constant for all points.
[20] R. Heitz *et al.,* Phys. Rev. Lett. **83**, 4654 (1999).